The Journal of Eukaryotic Microbiology

ISOP Published by the International Society of Protistologists

Journal of Eukaryotic Microbiology ISSN 1066-5234

ORIGINAL ARTICLE

Molecular Phylogenetic Positions and Ultrastructure of Marine Gregarines (Apicomplexa) *Cuspisella ishikariensis* n. gen., n. sp. and *Loxomorpha* cf. *harmothoe* from Western Pacific scaleworms (Polynoidae)

Davis Iritani[a], Takeo Horiguchi[a] & Kevin C. Wakeman[b,c]

a Faculty of Science, Hokkaido University, North 10, West 8, Sapporo 060-0810, Japan
b Graduate School of Science, Hokkaido University, North 10, West 8, Sapporo 060-0810, Japan
c Institute for International Collaboration, Hokkaido University, Sapporo 060-0815, Japan

Keywords
Eugregarinorida; molecular phylogeny; parasite.

Correspondence
K.C. Wakeman, Graduate School of Science, Hokkaido University, North 10, West 8, Sapporo, 060-0810, Japan
Telephone number: +81117062738;
FAX number: +81-11-706-4851;
e-mail: wakeman.kevin@gmail.com

Received: 30 October 2017; revised 23 January 2018; accepted January 25, 2018. Early View publication February 21, 2018

doi:10.1111/jeu.12509

ABSTRACT

Marine gregarines are unicellular parasites of invertebrates commonly found infecting the intestine and coelomic spaces of their hosts. Situated at the base of the apicomplexan tree, marine gregarines offer an opportunity to explore the earliest stages of apicomplexan evolution. Classification of marine gregarines is often based on the morphological traits of the conspicuous feeding stages (trophozoites) in combination with host affiliation and molecular phylogenetic data. Morphological characters of other life stages such as the spore are also used to inform taxonomy when such stages can be found. The reconstruction of gregarine evolutionary history is challenging, due to high levels of intraspecific variation of morphological characters combined with relatively few traits that are taxonomically unambiguous. The current study combined morphological data with a phylogenetic analysis of small subunit rDNA sequences to describe and establish a new genus and species (*Cuspisella ishikariensis* n. gen., n. sp.) of marine gregarine isolated from the intestine of a polynoid host (*Lepidonotus helotypus*) collected from Hokkaido, Japan. This new species possesses a set of unusual morphological traits including a spiked attachment apparatus and sits on a long branch on the molecular phylogeny. Furthermore, this study establishes a molecular phylogenetic position for *Loxomorpha* cf. *harmothoe*, a previously described marine gregarine, and reveals a new group of gregarines that infect polynoid hosts.

GREGARINES are a group of understudied parasites that inhabit the digestive tracts and coelomic spaces of various invertebrate hosts. Marine gregarines are especially of interest due to their basal phylogenetic position on the apicomplexan tree. These lineages have retained plesiomorphic traits from the origin of the Apicomplexa and many extant species display key characteristics including monoxeny, conspicuous feeding stages, and myzocytosis (Leander 2008). Furthermore, marine gregarines are highly prevalent throughout the ocean, but most species remain undiscovered or are ambiguously represented in molecular datasets as environmental sequences (Leander 2008; Rueckert et al. 2011a; Sitnikova and Shirokaya 2013). Thus, one of the primary tasks in this field is to explore the poorly understood diversity of gregarines and reconcile their taxonomy with molecular phylogenetic data. These efforts, however, are often stifled by high levels of morphological variability, convergence onto similar morphologies, and molecular datasets that are unresolved due to quickly evolving regions along the ribosomal operon (Rueckert et al. 2010, 2011b; Wakeman and Leander 2012, 2013a).

Gregarines are mainly characterized through a combination of morphological, life history, and small subunit rDNA (SSU rDNA) data. For instance, the gregarine life cycle involves a conspicuous feeding stage known as the trophozoite which has numerous taxonomic characters including the arrangement of cortical microtubules, attachment

apparatuses, overall shape, and in some cases the capacity for asexual reproduction known as merogony (e.g. Leander 2006; Rueckert et al. 2013; Schrével et al. 2016; Simdyanov et al. 2017; Wakeman and Leander 2012, 2013b). Marine gregarine systematics is concerned mainly with this trophozoite stage as other life cycle stages are difficult to find in the ocean in contrast to terrestrial gregarine systematics where oocysts and infectious stages are more commonly found. The host species and host compartment are also used for species delimitation. Gregarine infections have been mainly documented from the intestinal lumen of invertebrate hosts (e.g. Desportes and Schrével 2013; Levine 1977; Rueckert et al. 2015; Schilder and Marden 2006; Wakeman and Leander 2013a; Zuk 1987), but some gregarines infect coelomic spaces (e.g. urosporidians; Leander et al. 2006) and reproductive tracts (e.g. *Monocystis agilis*; Field and Michiels 2005) as well. The character traits mentioned above have been used to broadly classify the gregarines into three major groups: the archigregarines, eugregarines, and neogregarines (Adl et al. 2012; Grassé 1953; Leander 2008). The validity of each of these broad groupings is currently in question, with the continual discovery of new taxa and in the light of ever expanding SSU rDNA phylogenies.

Eugregarines (Eugregarinorida Léger 1900) encompass most marine gregarine taxa, but the relationships and basic classifications within the group remain poorly defined and somewhat contentious. Simdyanov et al. (2017) recently established a set of characters to define all eugregarines as a monophyletic group which includes the epimerite, epicytic crests, and gliding motility. On the other hand, other work has suggested that the varying forms among eugregarines are a consequence of convergent evolution from ancestral (archigregarine) lineages that have given rise independently to gregarines that are superficially similar (Wakeman and Leander 2012; Wakeman et al. 2014a,b). Discrepancies in higher level classification of gregarines is largely due to the difficulty in finding morphological characters that can be used to reliably infer evolutionary history. Evolutionary traits such as gliding motility, epimerites, and the submembrane architecture of surface folds are not clearly resolved on any molecular dataset and these traits tend to vary extensively even among seemingly closely related individuals (Rueckert et al. 2013; Simdyanov et al. 2017; Wakeman and Leander 2012; Wakeman et al. 2014a,b). The distribution of these types of traits causes uncertainty in the integrity of the eugregarines as a valid grouping and will require more comprehensive datasets detailing novel morphological forms and molecular diversity to fully resolve eugregarine systematics. The discovery of new subclades and comprehensive characterization of new species through integration of SSU rDNA data with morphological data, however, has contributed to progress towards a better understanding of eugregarine evolution (Rueckert et al. 2010, 2013).

In the present study, we describe a new species of aseptate marine eugregarine with a spiky attachment apparatus and apparent gigantism discovered from a scaleworm host in Japan. This new species possesses several uncommon morphological traits and is recovered on a divergent branch in a phylogenetic analysis of SSU rDNA sequences. A new genus was established to accommodate the new species based on host affiliation, comparative trophozoite morphology, and SSU rDNA phylogenetic analysis. Furthermore, we present and analyse the SSU rDNA from *Loxomorpha* cf. *harmothoe* (Hoshide 1988), a previously described marine gregarine (Hoshide 1988; Simdyanov 1996) also from a scaleworm host. This study is the first to sequence *Loxomorpha* cf. *harmothoe* and provide a molecular phylogenetic context for the scaleworm gregarines. The discovery of the new species and its unique morphology additionally helps to highlight some of the challenges associated with incorporating morphology to inform gregarine systematics and the usefulness of molecular data in this endeavour.

MATERIALS AND METHODS

Collection of host material and isolation of gregarine trophozoites

The annelid hosts *Lepidonotus helotypus* (Grube 1877) and *Harmothoe imbricata* (Linnaeus 1767) were collected on 14 April 2017 from the rocky intertidal of Ishikari Bay, Hokkaido, Japan (43°13′35.0″N 141°00′58.3″E). The geography consists of a relatively sheltered bay with large, loose rocks scattered throughout the intertidal zone among patches of brown macroalgae. The hosts were collected by hand from the underside of rocks and were dissected on the same day.

Gregarine trophozoites were found in the intestine of the host worms. Each individual worm was placed in a Petri dish filled with filtered seawater and split longitudinally with fine forceps. The intestine was then extracted and torn open to spill the gut contents. Gregarine trophozoites were located among food particles and digestive debris using an Olympus CK40 (Olympus Corp. Tokyo, Japan) inverted microscope. Hand-drawn glass pipettes were used for individual cell isolations. Each trophozoite was washed three times with filtered seawater in a well slide before each was placed in its own 0.2 ml PCR tubes for subsequent SSU rDNA analysis. The remaining trophozoites were set aside for light microscopy (LM), scanning electron microscopy (SEM), and transmission electron microscopy (TEM).

Light microscopy

Trophozoite morphology was initially observed in differential interference contrast (DIC) with a Zeiss Axioskop 2 *Plus* microscope (Carl-Zeiss, Göttingen, Germany) paired to a Leica MC120 HD colour camera (Leica, Wetzlar, Germany). Light micrographs were edited with Adobe Photoshop 11.

Scanning electron microscopy

Cuspisella ishikariensis n. gen., n. sp. trophozoites were isolated from *Lepidonotus helotypus*. Trophozoites from the hosts were pooled and fixed for SEM using 24-well

tissue culture plates and plastic capsules to hold and move the trophozoites between fixation steps. The bases of 1,000 μl pipette tips were cut from the tapered ends, creating a hollow cylinder, and a 50-μm mesh was added to cover one of the open ends. The customized capsules were submerged in the wells of the tissue culture plates filled with 2.5% glutaraldehyde. Trophozoites were transferred to these capsules using hand-drawn glass pipettes. The trophozoites were left to fix in the glutaraldehyde for 30 min on ice. Each capsule holding the trophozoites was then moved to an adjacent well and was rinsed with filtered, chilled seawater and left to soak for 5 min. The capsules were moved to the next well filled with 1% OsO_4 and left to soak for 30 min on ice. Each capsule was rinsed and soaked again with filtered, chilled seawater. The trophozoites were then dehydrated in serial dilutions of ethanol by submerging the capsules for three minutes at 50%, 70%, 80%, 90%, and 100% dilutions. Following the ethanol baths, the capsules were placed in a Hitachi HCP-2 815B critical point dryer (Nissei Sangyo America, Ltd., Pleasanton, CA, USA). The mesh was then carefully peeled from the pipette tips and attached to SEM stubs using double-sided tape. Each stub was sputter coated with gold for 180 s at 15 μA. Scanning electron micrographs were taken on a Hitachi S3000N scanning electron microscope and edited with Adobe Photoshop 11.

Transmission electron microscopy

Trophozoites were fixed for TEM using plastic capsules like those described for the SEM fixations. The bases of 1,000 μl pipette tips were cut and one end was covered with a small piece of plastic projector transparency. The plastic capsules were then filled with filtered, chilled 2.5% glutaraldehyde. Several trophozoites were transferred from the host dissections to each capsule with hand-drawn glass pipettes. The trophozoites were left to fix in 2.5% glutaraldehyde for 30 min on ice. The glutaraldehyde was removed with three filtered seawater washes from the capsules with 5-min soaks between each wash. Following the washes, the cells were left to soak in 4% OsO_4 for 1.5 h on ice, in the dark. The OsO_4 was removed with three seawater washes with 5-min soaks in between each wash. The trophozoites were dehydrated in serial dilutions of ethanol for 5 min at 80%, 90%, and 100%. The ethanol was replaced with a 1:1 mixture of 100% ethanol and 100% acetone for five minutes. Cells were then left to soak in 100% acetone for three minutes. This was then replaced with a 1:1 mixture of 100% acetone and resin for 30 min. Subsequently, 100% resin was added to the capsule for 12 h. The resin was replaced with fresh resin and incubated at 65 °C to polymerize. All transmission electron micrographs were taken on a Hitachi H-7650.

DNA extraction, amplification, and sequencing

For each species, seven trophozoites were isolated, washed three times with filtered seawater, and placed in separate 0.2 ml PCR tubes. Genomic DNA was extracted from the single-cell isolates using a QuickExtract FFPE RNA Extraction Kit (Epicentre, Madison, WI, USA).

SSU rDNA sequences were initially amplified by a polymerase chain reaction (PCR) using universal eukaryote primers PF1 5′ – CGCTACCTGGTTGATCCTGCC – 3′ and SSUR4 5′ – GATCCTTCTGCAGGTTCACCTAC – 3′ (Leander et al. 2003). Template DNA and primer pairs were added to Econotaq 2× Mastermix (Lucigen Corp. Middleton, WI). The following thermal cycle was used: initial denaturation at 94 °C for 2 min followed by 35 cycles of denaturation at 94 °C for 30 s, annealing at 52 °C for 30 s, extension at 72 °C for 2:00 min, and a final extension at 72 °C for 5 min. For both species, the product from this initial amplification was used as the template for a second round of nested PCRs using internal primers 18SRF 5′ – CCCGTGTTGAGTCAAATTAAG – 3′ (Mo et al. 2002) and SR4 -AGGGCAAGTCTGGTGCCAG – 3′ (Yamaguchi and Horiguchi 2005). The products were screened on a 1% agarose gel and sequenced using the same primers as those used for the amplification and nested PCRs. Sequences were assembled using Geneious version 10.1.3 (Kearse et al. 2012) and initially identified by Basic Local Alignment and Search Tool (BLAST) analysis.

Molecular phylogenetic analyses

The phylogenetic positions of *Cuspisella ishikariensis* n. gen., n. sp. (1431 bp) and *L.* cf. *harmothoe* (1637 bp) were determined using a 78-taxon alignment of SSU rDNA sequences, including three dinoflagellate sequences (outgroup) and representatives from the major clades of apicomplexans. Sequences divergence between the single trophozoite isolations were 0.1% for *C. ishikariensis* n. gen., n. sp. and 2.8% for *L.* cf. *harmothoe*. Consensus sequences were used to represent *C. ishikariensis* n. gen., n. sp and *L.* cf. *harmothoe* in the molecular phylogenetic analysis. The taxa included in the final phylogenetic analysis were based on preliminary trees that were made using alignments built from a comprehensive set of available gregarine sequences. Clades on long branches (e.g. crustacean gregarines and *Trichotokara*) with little relevance to the phylogenetic position of *C. ishikariensis* n. gen., n. sp. and *L. harmothoe* were excluded from the final analysis for clarity. Two environmental sequences (KT814188 and KT812852) were also included in the analysis to verify that the SSU rDNA sequence from *C. ishikariensis* n. gen., n. sp. was accurate and not a chimeric sequence or artefact of PCR. The SSU rDNA sequences were aligned using the MAFFT algorithm (Katoh et al. 2002) on Geneious version 10.1.3 (Kearse et al. 2012). The MAFFT algorithm was chosen over others for its ability to account for the secondary structure of ribosomal subunits. Ambiguously aligned regions and gaps were cut from the final alignment using Aliscore version 2.0 (Kück et al. 2010; Misof and Misof 2009) and Alicut version 2.3. The resulting alignment included 1,464 unambiguously aligned sites.

The GTR+I+Γ model (proportion of invariable sites = 0.1780, gamma shape = 0.6940) was selected by

jModelTest version 2.1.10 (Darriba et al. 2012; Guindon and Gascuel 2003) for maximum likelihood and Bayesian analyses under the Akaike information criterion (AIC). The maximum likelihood (ML) tree and ML bootstrap values were calculated using RAxML version 8.2.10 (Stamatakis 2014) through the Cipres Science Gateway version 3.3 (Miller et al. 2010). Bayesian posterior probabilities were calculated using Mr. Bayes version 3.2.6 (Ronquist et al. 2012) using the GTR substitution model with invariable sites over a gamma distribution (lset nst = 6, rates = invgamma) and Monte Carlo Markov Chains (MCMC) run with the following parameters: 10,000,000 generations (ngen = 10,000,000), 2 runs (nruns = 2), 4 chains (nchains = 4), temperature parameter at 0.2 (temp = 0.200), sample frequency of 100, prior burn-in of 0.25 of sampled trees, and a stop rule of 0.01 to terminate the program when the split deviation fell below 0.01.

RESULTS

Cuspisella ishikariensis n. gen., n. sp

Trophozoites were brass-coloured and roughly rhomboidal with an anterior region ending at an attachment apparatus covered in superficial spikes ($n = 40$; Fig. 1A,B). The attachment apparatus on some trophozoites was observed to decrease in volume on occasion leaving the trophozoite with a flattened anterior end (Fig. 1C). Cross sections of the attachment apparatus viewed under TEM did not reveal any invaginations of the membrane as might be seen if the attachment apparatus was being retracted as opposed to simply decreasing in volume. At its largest volume, the attachment apparatus measured 35 to 117 μm in length ($\bar{X} = 67$ μm, $n = 40$) and 12 to 48 μm ($\bar{X} = 30$ μm, $n = 40$) in width and possessed rows of uniform, superficial spikes that pointed posteriorly between longitudinal rows of epicytic folds (Fig. 1D). The cells ranged between 303 to 851 μm ($\bar{X} = 498$ μm, $n = 40$) in length and 43 to 134 μm ($\bar{X} = 76$ μm, $n = 40$) in width. The nucleus was oval with a major axis of 24 to 57 μm ($\bar{X} = 37$ μm, $n = 40$) and a minor axis of 18 to 57 μm ($\bar{X} = 30$ μm, $n = 40$). The trophozoites were covered by longitudinal epicytic folds at a density of 4 to 5 folds/μm along the main body of the cell and 1 to 2 folds/μm along the attachment apparatus (Fig. 1E,F). No gliding motility was seen in the trophozoite stages and syzygy was observed to be lateral in one specimen under light microscopy. An attempt was made to isolate this pair of gregarines in syzygy, but the cells separated in the process and no micrographs could be taken.

Transmission electron microscopy revealed a cytoplasm containing mitochondria, Golgi bodies, amylopectin granules, and dense granules (Fig. 2). The mitochondria were large, often reaching lengths of approximately 10 μm (Fig. 2A–C), and branched in numerous places. Amylopectin granules and dense granules were distributed homogenously throughout the trophozoite. The spikes of the attachment apparatus appeared to form by inflation of a regular epicytic fold with cytosol (Fig. 2A). Some intermediary spikes were also observed adjacent to fully formed epicytic folds. At the posterior end, bacteria were found inhabiting the grooves between the epicytic folds (Fig. 2D). The grooves of the epicytic folds were also infrequently the site for cell inclusion (Fig. 2E). Microtubules were roughly arranged in rows and could only be found inside the attachment apparatus (Fig. 3A–C). Cross sections and longitudinal section posterior to the attachment apparatus did not reveal microtubules (Fig. 3D).

Loxomorpha cf. *harmothoe*

Trophozoite morphology was consistent with the original descriptions of *Loxomorpha harmothoe* (see Hoshide 1988 and Simdyanov 1996). The cells were elongate and cylindrical, measuring approximately 150 μm in length, 40 μm in width, and syzygy was caudofrontal (Fig. 4A). *Loxomorpha* cf. *harmothoe* also possessed an attachment apparatus upon which only epicytic folds, and no apparent spikes, could be seen in TEM sections (Fig. 4B). No dense arrays of microtubules were found in the attachment apparatus, although it has been previously suggested that microtubules are present in the body of *L. harmothoe* (Simdyanov 1996). Other organelles found within the cytoplasm included mitochondria, amylopectin granules, and dense granules (Fig. 4C–E).

Molecular phylogenetic analyses of SSU rDNA sequences

The 73-taxon alignment of SSU rDNA sequences yielded a strongly supported outgroup of dinoflagellates (93 maximum likelihood bootstrap [MLB], 1.00 Bayesian posterior probability [BPP]) and an ingroup of apicomplexans with a poorly resolved backbone (Fig. 5). Both maximum likelihood and Bayesian analyses recovered identical tree topologies. The apicomplexan backbone gave rise to piroplasmid, coccidian, rhytidocystid, cryptosporidian, and gregarine clades. The archigregarines were paraphyletic with *Platyproteum vivax* and *Filipodium phascolosomae* forming the most basal apicomplexan branch. Two distinct terrestrial gregarine clades were recovered: terrestrial gregarine clade I (74 MLB, 1.00 BPP) and terrestrial gregarine clade II (100 MLB, 1.00 BPP). Terrestrial gregarine clade I included environmental sequences (AF372779 and AY179988) acquired from marine environmental PCR surveys. Terrestrial gregarine clade II was comprised exclusively by gregarines described from terrestrial hosts. The marine gregarines include the capitellid gregarines, urosporids, lecudininds, *Difficilina*, *Veloxidium*, paralecudinids, *Selenidium*, polynoid gregarines, and sipunculid gregarines. Each group of marine gregarines was composed of members that infect similar hosts (e.g. capitellid gregarines and *Lankesteria* collected from tunicates).

Cuspisella ishikariensis n. gen., n. sp. (MF537615) was recovered on its own branch separate from a strongly supported lineage constituted by *Loxomorpha* cf. *harmothoe* (MF537616) and unidentified environmental sequences (KT814188 and KT812852). The two gregarine sequences and two environmental sequences grouped together on a

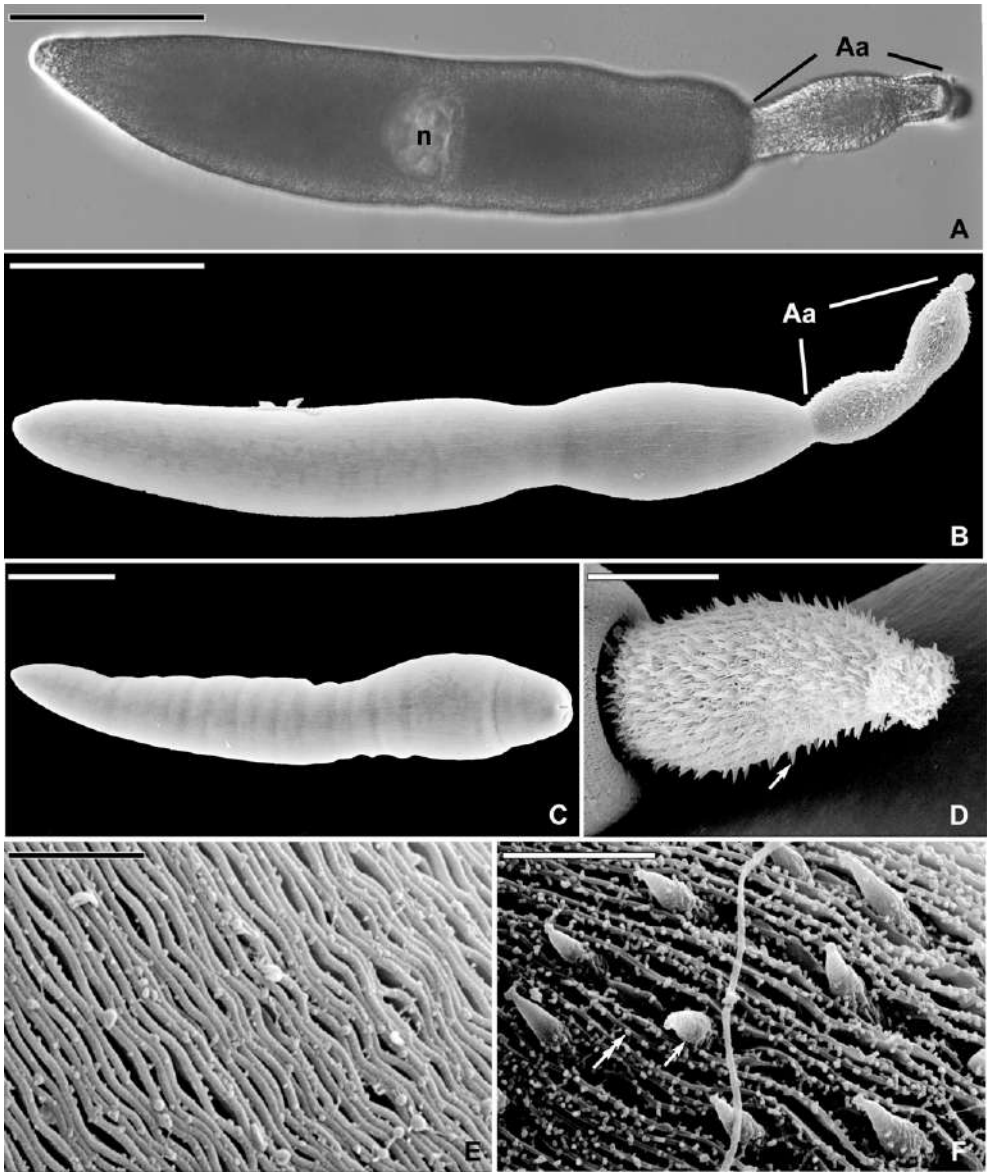

Figure 1 Light micrograph (LM) and scanning electron micrographs (SEM) of *Cuspisella ishikariensis* n. gen., n. sp. showing trophozoite morphology and ultrastructure. **(A)** LM of trophozoite taken in differential interference contrast (DIC). An oval nucleus (n) is visible located centrally within the cell. The attachment apparatus (Aa) is covered by spikes. **(B)** SEM of the trophozoite showing general trophozoite morphology and an attachment apparatus (Aa). **(C)** SEM of a trophozoite with a flattened anterior end due to the attachment apparatus having minimized in volume. **(D)** SEM close-up of the attachment apparatus. Superficial spikes (arrow) form longitudinal rows along the entire attachment apparatus in between epicytic folds. **(E)** SEM close-up of epicytic folds taken from the mid region of the trophozoite. **(F)** SEM close-up of the spikes (arrow) and epicytic folds (double-headed arrow) that line the attachment apparatus. *Scale bars*: A, B, C = 100 μm; D = 20 μm; E = 3 μm; F = 5 μm.

branch distinct from previously established marine gregarine clades (67 MLB, 1.00 BPP).

DISCUSSION

Molecular phylogenetic analyses of SSU rDNA sequences recovered a clade composed of two environmental sequences, *L.* cf. *harmothoe*, and *C. ishikariensis* n. gen., n. sp. The environmental sequences were used to verify that the SSU rDNA sequence used for *C. ishikariensis* was accurate, and not a product of chimerism or an artefact of PCR. *Loxomorpha harmothoe* was orignially described from the intestine of the polynoid host *Harmothoe imbricata* using light and electron microscopy (Hoshide 1988; Simdyanov 1996). The trophozoites of *L. harmothoe* are elongate and cylindrical (200 μm × 15 μm) ending in an anterior attachment apparatus and sexual reproduction occurs through caudofrontal syzygy. Due to the lack of genetic data in the original description of *L. harmothoe*, no comparison could be made between

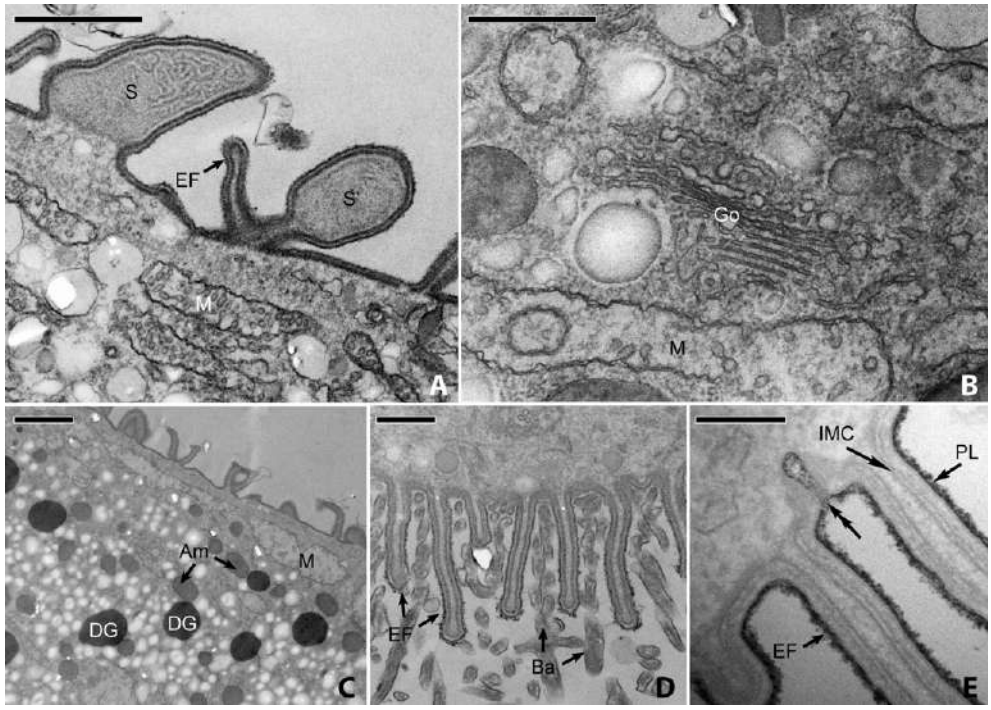

Figure 2 Transmission electron micrographs (TEM) of *Cuspisella ishikariensis* n. gen., n. sp. showing general subcellular morphology. Abbreviations: amylopectin granules (am), bacteria (Ba), dense granules (DG), epicytic fold (EF), Golgi body (Go), inner membrane complex (IMC), mitochondria (M), plasmalemma (PL), spike (S), developing/intermediary spikes (S'). **(A)** Longitudinal section showing the internal and surface morphology of the attachment apparatus. A fully formed spike (S) is seen next to one resembling an intermediary between a spike and an epicytic fold (S'). Inflation of an epicytic fold with cytosol may be the mechanism by which the spikes (S) form. **(B)** High magnification view of the organelles in the trophozoite body. **(C)** Longitudinal section showing a large mitochondrion near the periphery of the cell. **(D)** Longitudinal section taken from the most posterior end of the trophozoite. Bacteria are found in the grooves between the epicytic folds of the gregarine parasite. **(E)** High magnification view of the trophozoite plasmalemma and inner membrane complex. The open invagination of the plasma membrane through the IMC (double-headed arrows) is covered by a cell coat similar to that observed in Fig. 3C. *Scale bars*: A = 1 μm; B = 500 nm; C = 2 μm; D = 500 nm, E = 200 nm.

the SSU rDNA sequences of *L. harmothoe* (original description) and *L.* cf. *harmothoe* (this study). We have therefore continually distinguished the two throughout the text. *Cuspisella ishikariensis* n. gen., n. sp. was found in Hokkaido, Japan, the same locality as *L.* cf. *harmothoe*, from the intestine of the polynoid host *Lepidonotus helotypus*. Both species share basic morphological similarities such as an anterior region ending with an attachment apparatus as well as the lack of gliding motility in the trophozoite stages. In stark contrast, however, is the size difference between the trophozoites of *C. ishikariensis* n. gen., n. sp. (500 μm × 80 μm) and those of *L.* cf. *harmothoe* (150 μm × 40 μm). Syzygy in *C. ishikariensis* n. gen., n. sp. is also lateral and not caudofrontal. Intracellular differences are also clear whereby *C. ishikariensis* n. gen., n. sp. possesses large, branching mitochondria and a dense array of microtubules that support the attachment apparatus, whereas TEM sections of *L.* cf. *harmothoe* did not reveal any apparent microtubules arrays. Simdyanov (1996) reported the presence of microtubules in *L. harmothoe* through TEM micrographs, but they were more sparsely distributed than as seen in *C. ishikariensis* n. gen., n. sp. The attachment apparatus of *C. ishikariensis* n. gen., n. sp. was also covered by distinctive spikes arranged in rows, whereas the attachment apparatus of *L.* cf. *harmothoe* appeared to lack these spikes under thin sections viewed under TEM. The SEM photos taken by Simdyanov (1996) of *L. harmothoe* also did not show spikes projecting from the attachment apparatus, but we are unable to dismiss the possibility that the TEM sections and SEM micrograph by Simdyanov simply missed these structures due to rarity or small size.

The molecular phylogenetic analysis is consistent with the morphological differences in that the SSU rDNA sequences grouped the polynoid gregarines together, but clearly separated *C. ishikariensis* n. gen., n. sp. from *L.* cf. *harmothoe*. The combination of morphological and genetic differences, therefore, suggests that *C. ishikariensis* n. gen., n. sp. is a distinct species that also does not conform to the descriptions of *Loxomorpha* in general. Whether the grouping of *C. ishikariensis* n. gen., n. sp and *L. harmothoe* in the current analysis suggests a clade of gregarines that infect polynoid hosts in nature is unclear. Until a more comprehensive set of polynoid gregarines are characterized, the possibility that multiple gregarine clades infect polynoid hosts remains open.

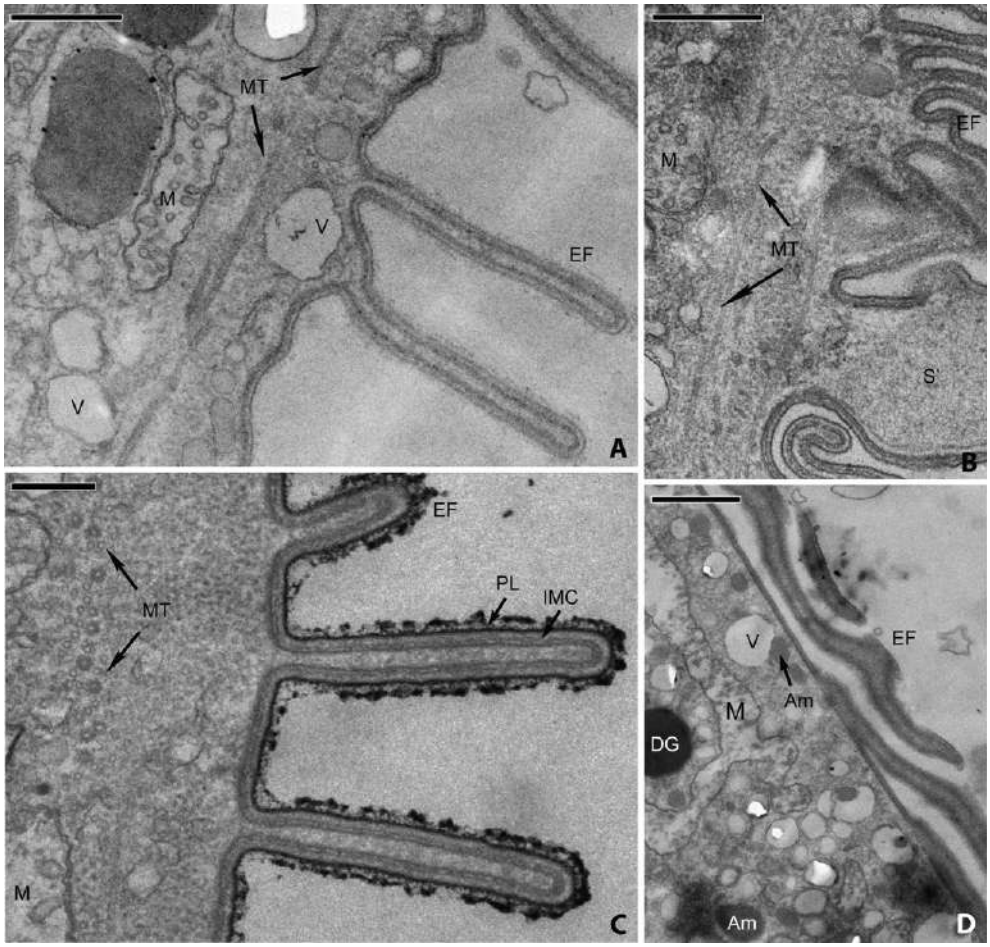

Figure 3 Transmission electron micrographs (TEM) of *Cuspisella ishikariensis* n. gen., n. sp. showing general subcellular morphology and microtubules. Abbreviations: amylopectin granules (Am), dense granules (DG), epicytic fold (EF), inner membrane complex (IMC), mitochondria (M), microtubules (MT), plasmalemma (PL), developing/intermediary spike (S'), and vacuoles (V). **(A)** Longitudinal section of an inflated attachment apparatus showing dense arrays of microtubules. **(B)** Longitudinal section taken from the anterior end of an inflated attachment apparatus showing microtubules beside a developing superficial spike. **(C)** Cross section of an inflated attachment apparatus showing a dense array of microtubules roughly arranged into rows. The plasmalemma and inner membrane complex are also visible. **(D)** Longitudinal section of trophozoite body posterior to the attachment apparatus. Subcellular components such as vacuoles, amylopectin granules, and dense granules are visible. Microtubules are not found in this region of the trophozoite. *Scale bars*: A, B = 500 nm; C = 250 nm; D = 1 μm.

Many original descriptions of gregarines are based on line drawings and lack molecular data. However, gregarine trophozoites often take on a great deal of intraspecific variation (e.g. the diverse morphotypes of *Paralecudina polymorpha* and *Lecudina* cf. *tuzetae*; Leander et al. 2003; Rueckert et al. 2011b) associated with motility (e.g. *Pterospora schizosoma*; Leander et al. 2006) and morphology of different developmental stages. As such, morphological traits are sometimes difficult to interpret and their plasticity can confound gregarine systematics in the absence of molecular data. The distinctiveness of *L. harmothoe* from the genus *Lecudina* was previously brought into question (Clopton 2000), but this study provides evidence based on SSU rDNA sequences that it does indeed belong to a separate genus. Comparative morphology and molecular phylogenetic analysis of SSU rDNA further suggests that *C. ishikariensis* n. gen., n. sp. is a novel species belonging to its own genus. Moreover, this study is the first to establish a molecular phylogenetic position for the *L.* cf *harmothoe* and *C. ishikariensis* n. gen., n. sp.

The molecular phylogenetic pattern whereby closely related gregarines infect closely related hosts is seen consistently across marine gregarine taxa (Iritani et al. 2017; Rueckert et al. 2015; Wakeman and Leander 2013a,b). Such phylogenetic association of gregarine parasites and their host set shows that gregarines have co-evolved with their invertebrate hosts to yield a level of host specificity. In contrast to this pattern, some gregarine species have diversified sympatrically within a host as in the case of *Selenidium melongena* and *S. terebellae;* two sister species that simultaneously infect the coelom and intestinal lumen respectively. Co-evolutionary phylogenetic patterns

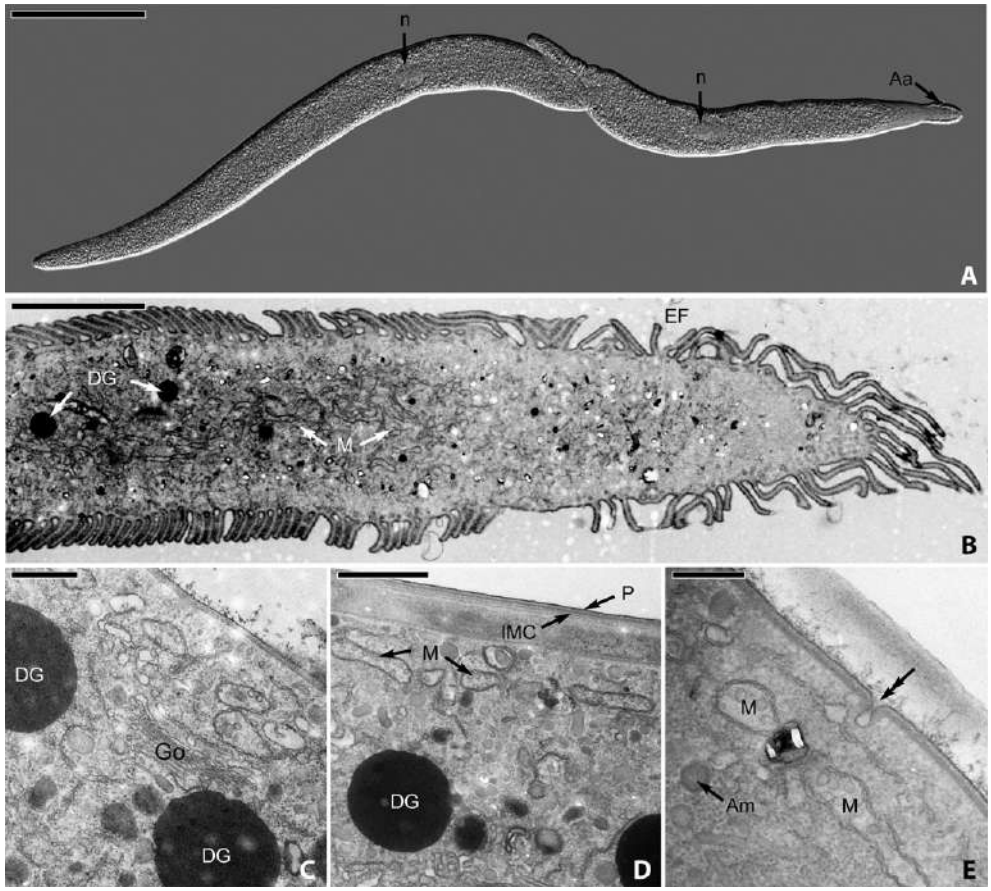

Figure 4 Light micrograph (LM) and transmission electron micrographs (TEM) of *Loxomorpha* cf. *harmothoe*. **(A)** LM of trophozoite taken in differential interference contrast (DIC). The cylindrical trophozoite possesses an oval nucleus (n) that is visible and located centrally within the cell. An attachment apparatus (Aa) is also apparent, but is not covered by spikes as seen in *Cuspisella ishikariensis* n. gen., n. sp. Syzygy is caudofrontal. **(B)** Longitudinal section taken through the attachment apparatus. Epicytic folds (EF) cover the outer surface of the cell and mitochondria (M) and dense granules (DG) are seen in the cytoplasm. There are no visible arrays of densely arranged microtubules. The attachment apparatus is also devoid of spikes and is instead covered exclusively in typical epicytic folds. **(C)** Longitudinal section of the trophozoite body posterior to the attachment apparatus with an apparent Golgi body (Go) and dense granules (DG). **(D)** Longitudinal section of the trophozoite body showing the plasmalemma (P) and inner membrane complex (IMC). Mitochondria (M) are arranged near the periphery of the cell and large dense granules (DG) are visible. **(E)** A cell inclusion (double-headed arrow), amylopectin granules (Am), and mitochondria (M). *Scale bars*: A = 100 μm; B = 4 μm; C = 2 μm; D = 1 μm; E = 500 nm.

in gregarine systematics are not evident from comparative morphology alone, which highlights the indispensable role molecular phylogenetic data play for further elucidating gregarine diversity and evolutionary history.

TAXONOMIC SUMMARY

Phylum Apicomplexa Levine, 1970
Order Eugregarinorida Léger, 1900
Cuspisella n. gen. Iritani, Horiguchi, and Wakeman 2017
Description. Trophozoites are long and roughly rhomboidal. A conspicuous attachment apparatus, which can decrease in volume, is uniformly covered in spikes arranged in longitudinal rows. Microtubules are present only in the attachment apparatus. Epicytic folds run along the length of the cell and become less dense on the attachment apparatus. Syzygy is lateral. Trophozoites do not display gliding motility.
Type Species. *Cuspisella ishikariensis*
Etymology. The genus name refers to the small (Latin: -*ella*) spike (Latin: *Cuspis*-) found on the attachment apparatus of the type species.
Cuspisella ishikariensis n. sp. Iritani, Horiguchi, and Wakeman 2017
Description. Trophozoites are brass-coloured and roughly rhomboidal ranging between 303 to 851 μm in length and 43 to 134 μm in width. Anterior region ends with attachment apparatus lined with superficial spikes. Attachment apparatus can decrease in volume leaving a flattened anterior end on some trophozoites. Attachment apparatus measures 35 to 117 μm in length and 12 to 48 in width and is supported by microtubules. Nucleus is oval with a

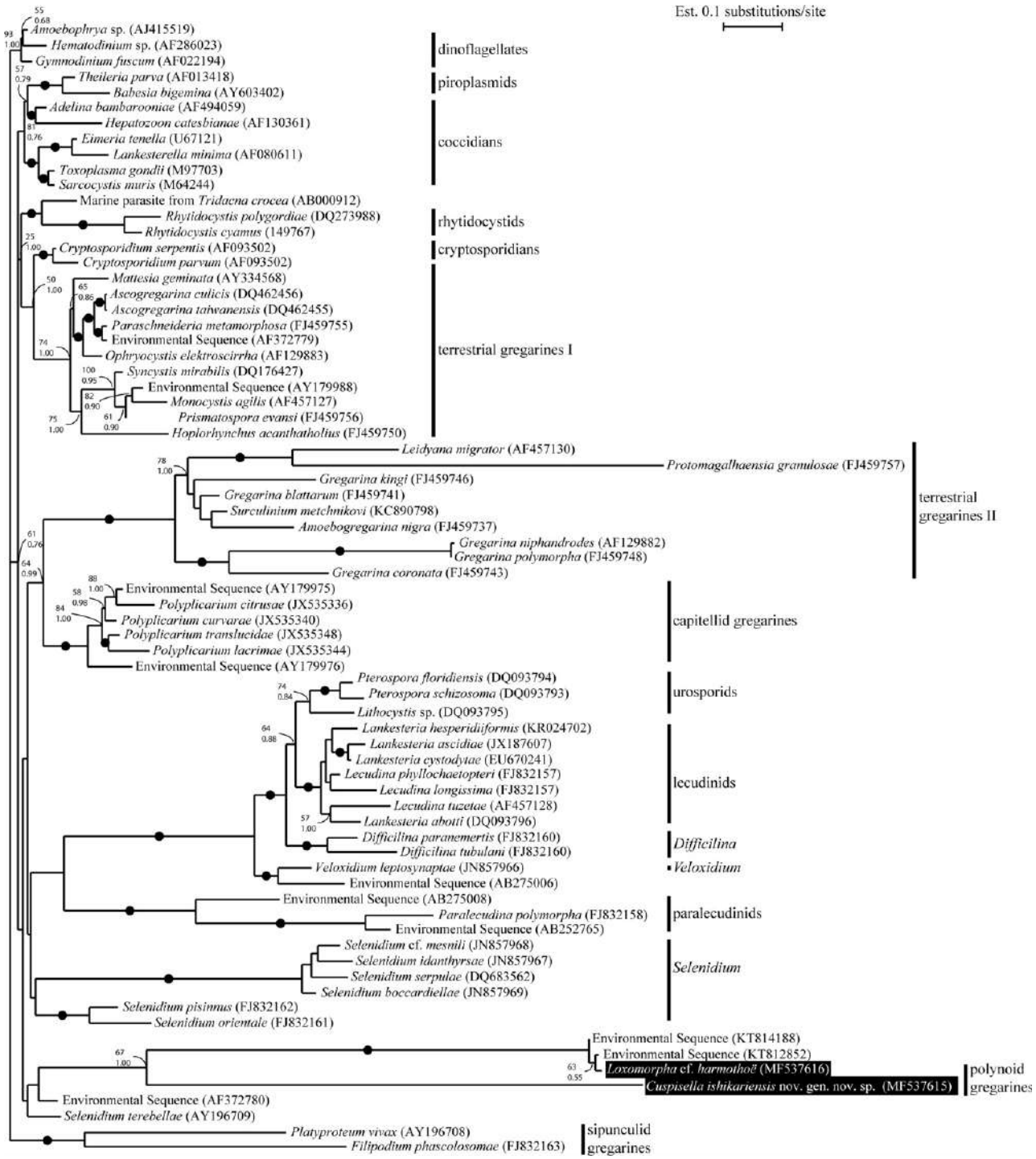

Figure 5 Maximum likelihood tree inferred from a 78 taxa dataset of SSU rDNA sequences with 1,464 unambiguously aligned sites using the GTR+I+ Γ model of substitution (gamma shape = 0.6940, proportion of invariable sites = 0.1780). Numbers denote support values with the top values indicating bootstrap support and the bottom indicating Bayesian posterior probabilities. The black dots were used on branches when both bootstrap support and Bayesian posterior probabilities were equal to or > 95 and 0.99 respectively. Support values were excluded from this tree when both bootstrap support and Bayesian posterior probabilities fell below 55 and 0.95 respectively for any given branch. The new species described in the current study as well as the sequence for *Loxomorpha* cf. *harmothoe* is highlighted with a black box.

major axis of 24 to 57 μm and a minor axis of 18 to 57 μm. Large and occasionally branching mitochondria distributed throughout cytoplasm. Longitudinal epicytic folds line the trophozoite at 4 to 5 folds/μm and 1 to 2 folds/μm along the attachment apparatus. Trophozoites display no gliding motility and syzygy is lateral.

DNA sequence. SSU rDNA sequence (GenBank MF537615).

Type locality. Ishikari Bay, Hokkaido, Japan (43°13′35.0″N 141°00′58.3″E). Host commonly found on the underside of large (~1 m diameter) rocks in the low intertidal to subtidal zones.

Type habitat. Marine

Type host. *Lepidonotus helotypus* Grube, 1877 (Annelida, Polychaeta, Phyllodocida, Polynoidae).

Location in host. Intestinal lumen

Iconotype. Fig. 1A

Hapantotype. Trophozoites on SEM stubs with a gold/palladium alloy sputter coat have been stored in the algal and protist collection in the Hokkaido University Museum (DI – 1).

LSID. 69E7303B-03E0-480A-9250-965200061B6A

Etymology. The species name refers to the type locality of Ishikari Bay

ACKNOWLEDGMENTS

This research was supported by a MEXT Doctoral Scholarship to Davis Iritani, as well as start-up funding from the International Institute for Collaboration at Hokkaido University and a joint JSPS/MBIE-RSZN provided to Kevin Wakeman.

LITERATURE CITED

Adl, S. M., Simpson, A. G. B., Lane, C. E., Lukeš, J., Bass, D., Bowser, S. S., Brown, W., Burki, F., Dunthorn, M., Hampl, V., Heiss, A., Hoppenrath, M., Lara, E., Le Gall, L., Lynn, D. H., McManus, H., Mitchell, E. A. D., Mozley-Stanridge, S. E., Parfrey, L. W., Pawlowski, J., Rueckert, S., Shadwick, L., Schoch, C. L., Smirnov, A. & Spiegel, F. 2012. The revised classification of eukaryotes. *J. Eukaryot. Microbiol.*, 59:429–493.

Clopton, R. E. 2000. Phylum Apicomplexa Levine, 1970: order Eugregarinorida Léger, 1900. *In*: Lee, J. J., Leedale, G., Patterson, D. & Bradbury, P. C. (ed.), Illustrated Guide to the Protozoa, 2nd edn. Society of Protozoologists, Lawrence, Kansas. p. 205–288.

Darriba, D., Taboada, R., Doallo, G. L. & Posada, D. 2012. jModelTest 2: more models, new heuristics and parallel computing. *Nat. Methods*, 9:772.

Desportes, I. & Schrével, J. 2013. The Gregarines. *In*: Desportes, I. & Schrével, J. (ed.),Treatise on Zoology-Anatomy, Taxonomy, Biology. Koninklijke Brill NV, Leiden. p. 197–389.

Field, S. G. & Michiels, N. K. 2005. Parasitism and growth in the earthworm *Lumbricus Terrestris*: fitness costs of the gregarine parasite *Monocystis* sp. *Parasitology*, 130:397–403.

Grassé, P. P. 1953. Classe Des Grégarinomorphes (Gregarinomorpha, n. nov., Grégarinae Haeckel, 1866; Grégarinidea Lankester, 1885; Grégarines Des Auteurs). *In*: Grassé, P. P. (ed.), Traité de Zoologie. Macon et cie, Paris. p. 590–690.

Guindon, S. & Gascuel, O. 2003. A simple, fast, and accurate algorithm to estimate large phylogenies by maximum likelihood. *Syst. Biol.*, 52:696–704.

Hoshide, K. 1988. Two Gregarines found in polychaetes from the Hokkaido Coast of Japan. *Proc. Jpn. Soc. Syst. Zool.*, 37:47–53.

Iritani, D., Wakeman, K. C. & Leander, B. S. 2017. Molecular phylogenetic positions of two new marine gregarines (Apicomplexa) - *Paralecudina anankea* n. sp. and *Lecudina caspera* n. sp. - from the intestine of *Lumbrineris inflata* (Polychaeta) show patterns of co-evolution. *J. Eukaryot. Microbiol.*, https://doi.org/10.1111/jeu.12462.

Katoh, K., Misawa, K., Kuma, K. & Miyata, T. 2002. MAFFT: a novel method for rapid multiple sequence alignment based on fast Fourier transform. *Nucleic Acids Res.*, 30:3059–3066.

Kearse, M., Moir, R., Wilson, A., Stones-Havas, S., Cheung, M., Sturrock, S., Buxton, S., Cooper, A., Markowitz, S., Duran, C., Thierer, T., Ashton, B., Meintjes, P. & Drummond, A. 2012. Geneious basic: an integrated and extendable desktop software platform for the organization and analysis of sequence data. *Bioinformatics*, 28:1647–1649.

Kück, P., Meusemann, K., Dambach, J., Thormann, B., Reumont, B. M., Wägele, J. W. & Misof, B. 2010. Parametric and non-parametric masking of randomness in sequence alignments can be improved and leads to better resolved trees. *Front. Zool.*, 7:10.

Leander, B. S. 2006. Ultrastructure of the Archigregarine *Selenidium vivax* (Apicomplexa) – A dynamic parasite of sipunculid worms (host: *Phascolosoma agassizii*). *Mar. Biol. Res.*, 2:178–190.

Leander, B. S. 2008. Marine gregarines: evolutionary prelude to the apicomplexan radiation? *Trends Parasitol.*, 24:60–67.

Leander, B. S., Harper, J. T. & Keeling, P. J. 2003. Molecular phylogeny and surface morphology of marine aseptate gregarines (Apicomplexa): *Selenidium* spp. and *Lecudina* spp. *J. Parasitol.*, 89:1191–1205.

Leander, B. S., Lloyd, S. A. J., Marshall, W. & Landers, S. C. 2006. Phylogeny of marine gregarines (Apicomplexa) - *Pterospora*, *Lithocystis* and *Lankesteria* - and the origin(s) of coelomic parasitism. *Protist*, 157:45–60.

Levine, N. D. 1977. Revision and checklist of the species (other than *Lecudina*) of the aseptate gregarine family lecudinidae. *J. Protozool.*, 24:41–52.

Miller, M. A., Pfeiffer, W. & Schwartz, T. 2010. Creating the CIPRES Science Gateway for Inference of Large Phylogenetic Trees. *2010 Gateway Computing Environments Workshop, GCE 2010*. https://doi.org/10.1109/GCE.2010.5676129.

Misof, B. & Misof, K. 2009. A Monte Carlo approach successfully identifies randomness in multiple sequence alignments: a more objective means of data exclusion. *Syst. Biol.*, 58:21–34.

Mo, C., Douek, J. & Rinkevich, B. 2002. Development of a PCR strategy for thraustochytrid identification based on 18S rDNA sequence. *Mar. Biol.*, 140:883–889.

Ronquist, F., Teslenko, M., Van Der Mark, P., Ayres, D. L., Darling, A., Höhna, S., Larget, B., Liu, L., Suchard, M. A. & Huelsenbeck, J. P. 2012. Mrbayes 3.2: efficient Bayesian phylogenetic inference and model choice across a large model space. *Syst. Biol.*, 61:539–542.

Rueckert, S., Chantangsi, C. & Leander, B. S. 2010. Molecular systematics of marine gregarines (Apicomplexa) from North-Eastern Pacific Polychaetes and Nemerteans, with descriptions of three novel species: *Lecudina phyllochaetopteri* sp. nov., *Difficilina tubulani* sp. nov. and *Difficilina paranemertis* sp. nov. *Int. J. Syst. Evol. Microbiol.*, 60:2681–2690.

Rueckert, S., Simdyanov, T. G., Aleoshin, V. V. & Leander, B. S. 2011a. Identification of a divergent environmental dna sequence clade using the phylogeny of gregarine parasites (Apicomplexa) from Crustacean Hosts. *PLoS ONE*, 6:e18163.

Rueckert, S., Villette, P. M. A. H. & Leander, B. S. 2011b. Species boundaries in gregarine apicomplexan parasites: a case study-comparison of morphometric and molecular variability in *Lecudina* cf. *tuzetae* (eugregarinorida, lecudinidae). *J. Eukaryot. Microbiol.*, 58:275–283.

Rueckert, S., Wakeman, K. C., Jenke-Kodama, H. & Leander, B. S. 2015. Molecular systematics of marine gregarine apicomplexans from Pacific tunicates, with descriptions of five novel species of *Lankesteria*. *Int. J. Syst. Evol. Microbiol.*, 65:2598–2614.

Rueckert, S., Wakeman, K. C. & Leander, B. S. 2013. Discovery of a diverse clade of gregarine apicomplexans (Apicomplexa: Eugregarinorida) from Pacific eunicid and onuphid polychaetes, including descriptions of *Paralecudina* n gen., *Trichotokara japonica* n. sp., and *T. eunicae* n. sp. *J. Eukaryot. Microbiol.*, 60:121–136.

Schilder, R. J. & Marden, J. H. 2006. Metabolic syndrome and obesity in an insect. *Proc. Natl Acad. Sci. USA*, 103:18805–18809.

Schrével, J., Valigurová, A., Prensier, G., Chambouvet, A., Florent, I. & Guillou, L. 2016. Ultrastructure of *Selenidium pendula*, the type species of archigregarines, and phylogenetic relations to other marine apicomplexa. *Protist*, 167:339–368.

Simdyanov, T. G. 1996. The morphology and ultrastructure of the gregarine loxomorpha harmothoë from the white sea. *Parazitologiya*, 30:174–180.

Simdyanov, T. G., Guillou, L., Diakin, A. Y., Mikhailov, K. V., Schrével, J. & Aleoshin, V. V. 2017. A new view on the morphology and phylogeny of eugregarines suggested by the evidence from the gregarine *Ancora sagittata* (Leuckart, 1860) Labbé, 1899 (Apicomplexa: Eugregarinida). *PeerJ*, 5:1–46.

Sitnikova, T. Y. & Shirokaya, A. A. 2013. New data on deep water Baikal limpets found in hydrothermal vents and oil-seeps. *Arch. für Molluskenkunde*, 142:257–278.

Stamatakis, A. 2014. RAxML version 8: a tool for phylogenetic analysis and post-analysis of large phylogenies. *Bioinformatics*, 30:1312–1313.

Wakeman, K. C., Heintzelman, M. B. & Leander, B. S. 2014a. Comparative ultrastructure and molecular phylogeny of *Selenidium melongena* n. sp. and *S. terebellae* Ray 1930 demonstrate niche partitioning in marine gregarine parasites (Apicomplexa). *Protist*, 165:493–511.

Wakeman, K. C. & Leander, B. S. 2012. Molecular phylogeny of Pacific archigregarines (Apicomplexa), including descriptions of *Veloxidium leptosynaptae* n. gen., n. sp., from the sea cucumber *Leptosynapta clarki* (Echinodermata), and two new species of *Selenidium*. *J. Eukaryot. Microbiol.*, 59:232–245.

Wakeman, K. C. & Leander, B. S. 2013a. Molecular phylogeny of marine gregarine parasites (Apicomplexa) from tube-forming polychaetes (Sabellariidae, Cirratulidae, and Serpulidae), including descriptions of two new species of *Selenidium*. *J. Eukaryot. Microbiol.*, 60:514–525.

Wakeman, K. C. & Leander, B. S. 2013b. Identity of environmental dna sequences using descriptions of four novel marine gregarine parasites, *Polyplicarium* n. gen. (Apicomplexa), from capitellid polychaetes. *Mar. Biodivers.*, 43:133–147.

Wakeman, K. C., Reimer, J. D., Jenke-Kodama, H. & Leander, B. S. 2014b. Molecular phylogeny and ultrastructure of *Caliculium glossobalani* n. gen. et sp. (Apicomplexa) from a Pacific *Glossobalanus minutus* (Hemichordata) confounds the relationships between marine and terrestrial gregarines. *J. Eukaryot. Microbiol.*, 61:343–353.

Yamaguchi, A. & Horiguchi, T. 2005. A further phylogenetic study of the heterotrophic dinoflagellate genus, *Protoperidinium* (Dinophyceae) based on small and large subunit ribosomal RNA gene sequences. *Phycological Res.*, 53:30–42.

Zuk, M. 1987. Seasonal and individual variation in gregarine parasite levels in the field crickets *Gryllus veletis* and *G. pennsylvanicus*. *Ecol. Entomol.*, 12:341–348.